# Collaborated Tasks-driven Mobile Charging and Scheduling: A Near Optimal Result

Tao Wu\*<sup>†</sup>, Panlong Yang\*, Haipeng Dai<sup>‡</sup>, Wanru Xu<sup>†</sup>, Mingxue Xu\*

\*School of Computer Science and Technology, University of Science and Technology of China

<sup>†</sup>College of Communication Engineering, Army Engineering University of PLA

<sup>‡</sup>State Key Laboratory for Novel Software Technology, Nanjing University, Nanjing, Jiangsu 210024, China
Email: {terence.taowu,xwr88023}@gmail.com, plyang@ustc.edu.cn, haipengdai@nju.edu.cn, xmx18@mail.ustc.edu.cn

Abstract-Wireless Power Transfer (WPT) has emerged into an inspiringly commercial and applicable era to charge devices. Existing studies mainly focus on general charging patterns and metrics while overlooking the collaborated task execution, which incurs charging inefficiency among nodes. In this paper we first advocate the collaborated tasks-driven mobile charging and scheduling to respect the energy requirement diversity. Specially, the mobile charging scheduling strategy is considered to maximize the overall task utility which concerns sensor selection and task cooperation. Unfortunately, solving this problem is non-trivial, because it involves solving two coupling NP-hard problems. In tackling with this difficulty, we construct a surrogate function with specific theoretical analysis of its submodularity and gap property. Then, we approximate the traveling cost to transform the formulated problem into an essentially monotone submodular function optimization subject to a general routing constraint, where we propose a (1-1/e)/4-approximation algorithm. Extensive simulations are conducted and the results show that our algorithm can achieve a near-optimal solution covering at least 84.9% of the optimal result achieved by the OPT algorithm. Furthermore, field experiments in office room and soccer field environment with 10 and 20 sensors are implemented respectively to validate our proposed algorithm.

## I. INTRODUCTION

Nowadays, wireless power transfer (WPT) has emerged into an inspiringly commercial and applicable era to charge devices due to the high reliability and efficiency of continuous power supply. These breakthroughs help enhance the energy transfer quality and encourage the application of wireless rechargeable sensor networks (WRSNs) [1].

Usually, rechargeable devices such as WISP tags are deployed in a certain area for executing a large number of sensing, computing, and communication tasks [2]. As there have been a large body of works on scheduling static chargers [3]–[9], we employ mobile chargers for energy replenishment due to the high mobility and flexibility for energy replenishment. Recent studies have mainly focused on general charging patterns and metrics to improve overall charging efficiency, which include extending network lifetime [10] [11], optimizing vacation time [12] [13], meeting on-demand [14], spatial and temporal charging requests [15] [16], minimizing charging delay [17], maximizing charging reward [18], etc. However, these schemes fall short in regarding charging effectiveness for task execution and cannot cater to the task-level energy requirement of sensors.

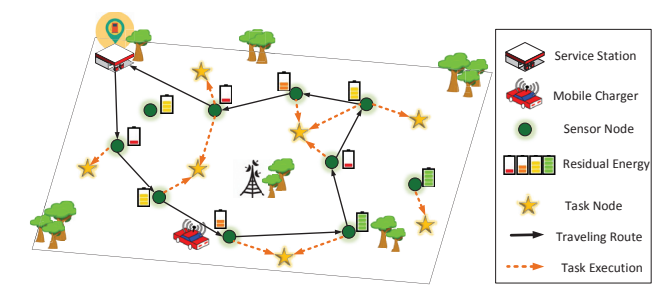


Fig. 1: The scenario of collaborated tasks-driven mobile charging

Nevertheless, many applications in sensor networks rely on the collaboration of tasks among nodes. a). In shared sensor networks with multi-application deployment such as urban sensing systems [19] and building automation [20], nodes are allowed to allocate resources to contending applications. Thus sensor nodes can participate in multiple tasks including temperature, humidity and radiation monitoring, security alarms, and light control based on their Quality of Monitoring of physical space [21]. b). In Software-Defined Sensor Network (SDSNs) that equipped by several different types of sensors [22], a sensor node is able to conduct multiple tasks with different sensing targets simultaneously and a given sensing task usually involves multiple sensors to achieve a certain quality of sensing. c). Besides, in event/target detection applications, spatially redundant or correlated data is generated due to the random deployment and high density of nodes [23] [24]. One sensor can detect multiple targets and one target is covered by multiple sensors.

Therefore, in this paper we investigate Collaborated Tasks-driven Mobile Charging (CTMC) problem. As shown in Fig. 1, we employ a mobile charger to replenish energy for partial energy-critical sensors to cooperate on specific tasks. One sensor may participate in executing (denoted by the dotted yellow line) multiple tasks and one task may be also accomplished by multiple sensors. Various sensors have various power consumptions and utility weights for task execution. Typically, the task can be the zone monitoring using directional cameras where the task utility (e.g., the *Quality of Monitoring*) is relevant to the distance, angle and allocated energy [25]. Thus we should devise a closed charging tour to maximize the overall task utility.

Our problem yields two main technical challenges:

- The first challenge is that selecting sensors for charging is a complex mixed integer programming mathematically, where the optimized objective function is nonlinear including the product of both integer and fractional variables.
- The second challenge is to schedule the charging tour of the mobile charger with constant energy budget, which is similar to a variant of the classic Traveling Salesman Problem (TSP) or the Orienteer Problem (OP). Generally, we cannot address this challenge individually because the two challenges are tightly coupled and make more complicated.

To address this difficulty, we construct a surrogate function to present the task cooperation for any selected sensors, which involves a greedy energy allocation strategy. Then, we approximate the charging tour using the nearest neighbour rule and transform the initial problem into maximizing a submodular function problem under a general routing constraint. We make the following three key contributions.

- First, we propose a novel energy allocation scheme for task cooperation. We prove the submodularity of the surrogate function and bound its theoretical gap comparing the optimal scheme.
- Second, we transform our initial problem and bound the performance loss with a (1-1/e)/4-approximation ratio by proposing an efficient Reward-Cost ratio (RC-ratio) algorithm.
- Third, we conduct extensive simulations and implement two field experiments using a TX91501 power transmitter and up to 20 rechargeable sensors to evaluate the performance of our algorithm. The results show that in terms of charging task utility, our algorithm can achieve a near-optimal solution covering at least 84.9% of the optimal result achieved by the OPT algorithm.

The rest of our paper is organized as follows. In Section II, we briefly survey related works. Then, we present our system model and problem formulation in Section III. We describe our solution in Section IV and theoretical analysis in Section V. Extensive simulations and field experiments are conducted in Section VI and VII, respectively. Finally, we conclude the paper in Section VIII.

# II. RELATED WORK

There are many research works on wireless charging using mobile chargers. Most of them focuses on relatively *general* charging patterns and metrics. For example, Peng et al. [10] designed a wireless charging system with the optimal charging sequence to maximize the network lifetime. Hou et al. [12] constructed a renewable energy cycle for sensor nodes. He et al. [14] considered the on-demand mobile charging and used a simple but efficient Nearest-Job-Next with Preemption discipline. Chi et al. [16] investigated the issue of multiple mobile chargers and considered the temporal and spatial requirements from charging requests. Fu et al. [17] proposed a proper algorithm to identify the optimal reader stop locations and corresponding stop durations to minimize the total charging

TABLE I: Definition of notations

Notation	Definition
$\overline{V}$	Set of sensors
$v_{j}$	Stationary sensor or location
m	Number of sensors
$e_j$	Battery capacity for sensor $v_j$
$e_j \\ e_j^r \\ c(v_j)$	Residual energy amount for sensor $v_j$
$c(v_j)$	Charging cost for sensor $v_j$
T	Set of tasks
$t_i$	Task
n	Number of tasks
$p_{ij}$	Allocated energy to task $t_i$ from sensor $v_j$
$w_{ij}$	Utility weight between task $t_i$ and sensor $v_j$
$u(t_i, v_j)$	Task utility from task $t_i$ by sensor $v_j$
$U_i$	Utility threshold for each task $t_i$
X	Sensor subset of $V$
$U(X,t_i)$	Task utility for single task $t_i$
E	Mobile charger energy capacity
P	Energy allocation strategy
U(X,P)	Overall task utility
$\mathcal{C}(.)$	Overall energy consumption
$\mathcal{C}^{\hat{T}\hat{S}P}(.)$	Traveling energy consumption
$c(v_j)$	Charging cost for sensor $v_j$
$\alpha, \beta$	Constants in the system model

delay. Zhao *et al.* [26] considered the design of joint energy replenishment and data gathering. They provided a selection algorithm to balance the energy replenishment amount and data gathering latency. Liang *et al.* [18] focused on the charging rewards maximization problem for full and partial charging. Zhou *et al.* [27] considered target k coverage in WRSNs and proposed a  $\lambda$ -GTSP charging algorithm after organizing sensors into load-balanced clusters. To the best of our knowledge, only Dong *et al.* [28] explicitly considered the task utility when introducing mobile charging. They considered a feasible task assignment in WRSNs to maximize the charger's velocity when a mobile charger traveled along a fixed routing to charge sensor nodes.

# III. SYSTEM MODEL AND PROBLEM FORMULATION

#### A. Network Model

We use  $V=\{v_1,v_2,...v_m\}$  to denote the set of m stationary rechargeable sensors distributed in a 2D plane. The set of associated n tasks is denoted by  $T=\{t_1,t_2,...t_n\}$ . Each sensor  $v_j$  is powered by a rechargeable battery with capacity  $e_j$ . Once sensors are selected for mobile charging, they exploit their harvested energy to execute tasks collaboratively. A mobile charger starts at the service station  $v_0$ , tries its best to charging sensor nodes and returns to the depot. We list the notations used as shown in Table I.

## B. Energy Consumption Model

For the energy consumption model, there are mainly two types of energy cost, the traveling energy cost and charging energy cost.  $(x[v_j], y[v_j])$  can be used to denote the location coordinate of this rechargeable sensor  $v_j$ . We consider the distance as a metric and then the Euclidean distance  $d:(V,V)\to \mathbf{R}$  between two sensors can be calculated.

Binary variable  $h_j$  is used to denote whether sensor  $v_j$  is selected for charging. For example,  $h_j$  is 1 if  $v_j$  is selected; otherwise, it is 0. Thus, for selected sensor set  $X \subseteq V$ , we

have  $h_j=1$  for each  $v_j\in X$  and obtain the following traveling energy cost

$$\mathcal{C}^{TSP}(X) = \sum_{d \in \mathcal{L}^{TSP}(X)} \alpha \cdot d.$$

 $\alpha$  is the energy consumption rate per unit length and  $\mathcal{L}^{TSP}(X)$  is a closed tour that starts and ends at the depot  $v_0$ , while all sensors in X are visited only once.

When considering the charging energy cost, we assume sensor  $v_j$  with capacity  $e_j$  has current residual energy  $e_j^r$ , then the amount of charging energy can be denoted by  $e_j - e_j^r$ . When charging sensors, there is energy loss inevitably which depends on the charging distances and angles. For simplicity, the mobile charger would consume  $\beta$  amount of energy when transferring one unit of energy to the sensor. Then, we denote the charging energy cost for sensor  $v_j$  as

$$c(v_j) = \beta \cdot (e_j - e_j^r).$$

Therefore, the overall charging energy cost for selected sensor set X is

$$\sum_{v_j \in X} c(v_j) = \sum_{v_j \in V} \beta(e_j - e_j^r) \cdot h_j, \quad \forall v_j \in X, h_j = 1.$$

Combining the consumed two energy cost during the charging tour, the total cost for any subset set X can be expressed as

$$\begin{split} \mathcal{C}(X) &= \mathcal{C}^{TSP}(X) + \sum_{v_j \in X} c(v_j) \\ &= \sum_{d \in \mathcal{L}^{TSP}(X)} \alpha \cdot d + \sum_{v_j \in V} \beta(e_j - e_j^r) \cdot h_j. \end{split}$$

## C. Task Utility Model

For the task utility model, we define the utility weight  $w_{ij}$  which means the achieved utility of unit power that sensor  $v_j$  spends on executing task  $t_i$ . Then, we have the task utility  $u(t_i, v_j)$  from sensor  $v_j$  to task  $t_i$  as

$$u(t_i, v_j) = w_{ij} p_{ij},$$

where  $p_{ij}$  is the amount of energy allocated to execute task  $t_i$  from sensor  $v_j$ . The utility of task contributed by multiple sensors is additive. That is, given any sensor set  $X \subset V$ , the total additive utility for task  $t_i$  can be calculated by

$$u_X(t_i) = \sum_{v_j \in X} u(t_i, v_j) = \sum_{v_j \in V} w_{ij} p_{ij} h_j.$$

 $h_j$  shows that only sensor  $v_j$  is selected by the mobile charger for charging could it allocate its achieved energy.

The maximum utility value of task  $t_i$  is represented by  $U_i$ . If the additive utility  $u_X(t_i)$  is larger than this threshold, the excessive utility *i.e.*,  $u_X(t_i) - U_i$  would be useless. Therefore, we have the final utility for task  $t_i$  as

$$U(X, t_i) = \min\{u_X(t_i), U_i\}.$$

## D. Problem Definition

Naturally, the overall task utility in the network is the sum for n tasks which is given by

$$U(X, P) = \sum_{i=1}^{n} U(X, t_i) = \sum_{i=1}^{n} \min\{u_X(t_i), U_i\}$$
  
=  $\sum_{i=1}^{n} \min\{\sum_{v_i \in V} w_{ij} p_{ij} h_j, U_i\}.$ 

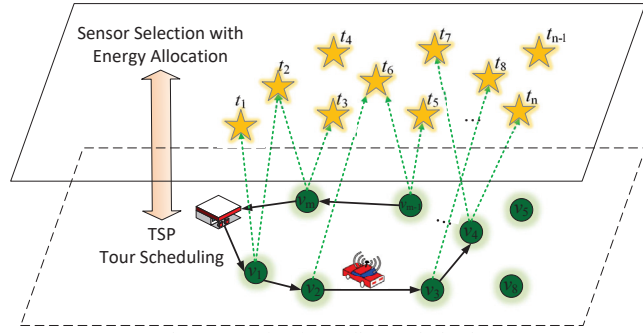


Fig. 2: Two-level coupling optimization

We use matrix variable  $P = \{p_{ij} | i = 1, ..., n; j = 1, ..., m\}$  to denote the energy allocation strategy for task cooperation. Since each sensor cannot be overloaded, the sum of allocated energy is no greater than the sensor capacity itself, then

$$e_j - \sum_{t_i \in T} p_{ij} h_j \ge 0 , \quad \forall v_j \in V.$$
 (1)

Meanwhile, the energy capacity of the mobile charger is limited and the total amount of energy consumption should not exceed the energy capacity E. Thus we also have

$$C(X) \le E, \quad \forall X \subseteq V.$$
 (2)

Based on above definitions and constraints, our object is to select a sensor subset X of V to find a closed charing tour with an energy allocation strategy P to maximize the overall task utility in the network. Therefore we can formulate the Collaborated Tasks-driven Mobile Charging (CTMC) problem as a mixed integer nonlinear programming problem.

$$\begin{array}{ll} \textbf{(CTMC)} \quad \text{Max} \quad U(X,P) \\ & \text{s.t.} \quad e_j - \sum\limits_{t_i \in T} p_{ij} h_j \geq 0 \;, \quad \forall v_j \in V \;\; (1) \\ & \quad \mathcal{C}(X) \leq E, \qquad \quad \forall X \subseteq V \;\; (2) \end{array}$$

 $h_j$  and  $p_{ij}$  are the variables that should be optimized to find X and P, respectively.

# A. Hardness Analysis

Based on the above problem definition, we can see that the CTMC problem includes the two-level optimization as shown in Fig. 2. The upper level optimization involves the sensor selection with energy allocation while the lower level optimization involves tour scheduling for these selected sensors.

While setting the traveling energy cost aside temporarily, the upper level problem can be regarded as a simplified version of the CTMC problem:

(CTMC-s) Max 
$$U(X, P)$$
  
s.t.  $e_j - \sum_{t_i \in T} p_{ij} h_j \ge 0$ ,  $\forall v_j \in V$  (1)  

$$\sum_{v_j \in V} \beta(e_j - e_j^r) \cdot h_j \le E, \ \forall v_j \in V$$
 (2.a)

Lemma 1: The upper level CTMC-s problem is NP-hard.

The proof of Lemma 1 is based on the reduction from the

The proof of Lemma 1 is based on the reduction from the *budget maximum coverage problem* [29], which is omitted due to the space limitation.

When considering the traveling energy cost, we can find that even computing the cost function C(X) is quite difficult

in many settings, since it involves finding a closed TSP tour  $\mathcal{L}^{TSP}(X)$ , which is NP-hard [30]. Apparently, the lower level tour scheduling is also NP-hard. Each optimization of one level problem would directly impact the other. Therefore, the upper and lower level optimizations in CTMC are coupled with each other and should not be addressed separately to obtain the global solution. Thus, the formulated CTMC problem is the combination of two coupling NP-hard problems.

### B. Surrogate Function Construction

Remember the objective function in the upper level optimization is nonlinear and related to optimal task cooperation. Then in this subsection we construct a surrogate function H(X) to approximate the nonlinear objective function.

Assuming we have selected sensor set X which does not violate the energy capacity constraint of the mobile charger. The set X has a random but fixed charging sequence. By devising a special energy allocation strategy, we can make the utility function to be linear. Then, our surrogate function H(X) could be regarded as a value mapping from set X to overall task utility. Based on this idea, we apply a greedy strategy to allocate energy of each sensor to cooperate on tasks according to the sequence in X as follows.

For sensor  $v_j$  in X, we sort the tasks according to the utility weight in a decreasing order. Then,  $v_j$  greedily allocates energy to various tasks in this order until each task improves up to the utility threshold or there is no energy left for allocation. In other words, we prefer to allocate energy as much as possible to execute the task that has the highest utility weight. Therefore, we could calculate task utility function value H(X) when given set X. Moreover, if we add a new sensor/element x into current set X, we always place x to the end of the sequence in X. And we allocate energy in the new set  $X' = X \cup \{x\}$  using the strategy above to obtain the function value H(X').

Our surrogate function H(X) is a special case of the initial objective function U(X,P). If we denote above energy allocation strategy by P', we then achieve the equational relation H(X) = U(X,P') and  $H_X(t_i) = U(X,t_i)$ . Additionally, we denote the optimal energy allocation method by  $P^*$  and the optimal task utility in the overall network can be represented by  $U(X,P^*)$ .

# C. Tour Scheduling Scheme

The lower level optimization in CTMC involves finding a shortest tour including partial sensors which ensures the total energy consumption not exceed the energy capacity E. Optimizing this energy consumption is similar to solving one variant of Traveling Salesman Problem (TSP), where it is often infeasible to compute the optimal cost. Thus, we could use an efficient approximate cost function  $\hat{\mathcal{C}}(X)$  to replace the optimal cost. We use  $\psi(m)$  to denote the approximation ratio when there is m sensors for selection. In our proposed algorithm, we just use a general and fast nearest neighbour rule to construct our TSP tour with a  $\log m$ -approximation [31]. The traveling cost approximation can influence the quality of utility approximation, which is described in next section.

#### D. Approximation Algorithm For CTMC

In this part, we jointly consider the two-level optimization and attempt to devise a simple but efficient approximation algorithm referring to the idea of [32].

Based on the approximation of TSP energy consumption, the core idea is to use the greedy method to iteratively select a new sensor  $v_j'$  which has the largest *reward-cost ratio* respecting the task utility. Then the sensor in iteration j is obtained as follows:

$$v_{j'} = \mathop{\arg\max}_{v \in V \backslash X_{j-1}} \frac{H(X_{j-1} \cup \{v\}) - H(X_{j-1})}{\hat{C}(X_{j-1} \cup \{v\}) - \hat{C}(X_{j-1})}.$$

 $v_0$  is the starting and ending point for the TSP tour. Initially,  $X_0=\emptyset$  and  $X_j=\{v_{1'},v_{2'},...,v_{j'}\}.$ 

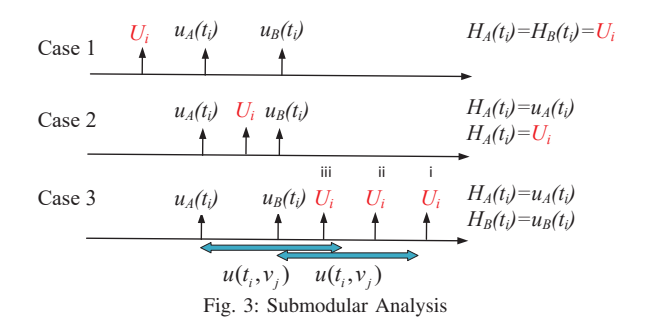
The progress of each iteration returns a better solution and the nature of our results will depend on the quality of TSP approximation. The details of the algorithm can be found in Algorithm 1. Solution X' only contains a single sensor. Utilizing this iterative method, we can add more sensors continuously until violating the energy capacity constraint of the mobile charger. We then find the sensor set  $X_j$ , where  $\hat{\mathcal{C}}(X_{j-1}) \leq E$  and  $\hat{\mathcal{C}}(X_j) \geq E$ . Finally we would compare H(X') with  $H(X_j)$  to select the maximal one.

# **Algorithm 1:** Reward-Cost ratio (RC-ratio)

```
Input: Task set T = \{t_1, t_2, ... t_n\}, starting point v_0, sensor set
              V = \{v_1, v_2, ... v_m\}, utility weight \{w_{ij}\}, charging
              energy budget E.
    Output: Sensor set X \subset V, energy allocation \{p_{ij}\}.
   Initialization. V' = V, j = 1, X_0 = \emptyset and \hat{\mathcal{C}}(X_0) = 0;
    X' = \arg\max\{H(v)|v \in V, \hat{\mathcal{C}}(v) \le E\};
 2 while V' \neq null do
          foreach v \in V' do
               Computing task utility H(X_{j-1} \cup \{v\}) and H(X_{j-1})
                with corresponding energy allocation scheme.
               Computing the approximate TSP energy consumption
               \hat{\mathcal{C}}(X_{j-1} \cup \{v\}) and \hat{\mathcal{C}}(X_{j-1}) using nearest neighbour
         v_{j'} = \underset{v \in V \setminus X_{j-1}}{\arg \max} \frac{H(X_{j-1} \cup \{v\}) - H(X_{j-1})}{\hat{\mathcal{C}}(X_{j-1} \cup \{v\}) - \hat{\mathcal{C}}(X_{j-1})}.
                  v \in \bar{V} \backslash X_{j-1}
          if C(X_{j-1} \cup \{v_j'\}) \leq E then
               X_j = X_{j-1} \cup \{\overline{v}'_j\}, \text{ return } p_{ij'};
              j=j+1;
         V' = V' \setminus v'_i;
10 if H(X') \ge H(X_{j-1}) then
    X = X';
12 else
13 X = X_{j-1};
14 Output X \subset V, \{p_{ij}\};
```

# V. THEORETICAL ANALYSIS

In this section, we give a series of theoretical analysis about the submodularity and gap property for the constructed surrogate function H(X) which helps transform our initial problem into a submodular maximization problem subject to



a general routing constraint. On this basis, we can prove the (1-1/e)/4 approximation ratio of the proposed algorithm.

#### A. Surrogate Function Properties Analysis

In this subsection, we prove our constructed surrogate function has three tractable properties: nonnegativity, monotonicity, and submodularity, which could be used to propose a bicriterion approximation algorithm as shown in Algorithm 1.

**Definition 1:** (Nonnegativity, Monotonicity, and Submodularity) Given a finite ground set  $\mathcal{U}$ , a real-valued set function is defined as  $f: 2^{\mathcal{U}} \to R$ , f is called *nonnegative*, *monotone* (nondecreasing), and submodular if and only if it satisfies following conditions, respectively.

- $f(\emptyset) = 0$  and  $f(A) \ge 0$  for all  $A \subseteq \mathcal{U}$  (nonnegative);
- $f(A) \le f(B)$  for all  $A \subseteq B \subseteq \mathcal{U}$  or equivalently:  $f(A \cup \{e\}) f(A) > 0$  for all  $A \subseteq \mathcal{U}$  and  $e \in \mathcal{U} \setminus A$  (monotone);
- $f(A) + f(B) \ge f(A \cup B) + f(A \cap B)$ , for any  $A, B \subseteq \mathcal{U}$  or equivalently:  $f(A \cup \{e\}) f(A) \ge f(B \cup \{e\}) f(B)$ ,  $A \subseteq B \subseteq \mathcal{U}$ ,  $e \in \mathcal{U} \setminus B$  (submodular);

Then, we have the following theorem:

**Theorem 2:** The constructed surrogate function is nonnegative, monotone and submodular.

*Proof:* According to the definition of our surrogate function,  $H(X) = U(X, P') \ge 0$ , then it is *nonnegative*.

When executing energy allocation strategy P', we have  $H_A(t_i) = U(A,t_i) = \min\{u_A(t_i),U_i\}$  and  $H_A(t_i) \leq H_B(t_i)$  for set  $A \subseteq B \subseteq V$ . According to the additive task utility model, we have the following equation

$$H(A) = \sum_{i=1}^{n} H_A(t_i) \le \sum_{i=1}^{n} H_B(t_i) = H(B)$$

that implies H(X) is monotone.

Here we give the specific explanation that H(X) is also submodular by proving  $H(A \cup \{v_j\}) - H(A) \ge H(B \cup \{v_j\}) - H(B)$ . It is equal to prove

$$H_{A \cup \{v_j\}}(t_i) - H_A(t_i) \ge H_{B \cup \{v_j\}}(t_i) - H_B(t_i).$$
 (3)

Fig. 3 presents three cases to give the proof.

(Case 1) If  $U_i \leq u_A(t_i) : H_B(t_i) \geq H_A(t_i)$ , we have

$$H_{A \cup \{v_i\}}(t_i) - H_A(t_i) = 0 = H_{B \cup \{v_i\}}(t_i) - H_B(t_i).$$

(Case 2) If  $u_A(t_i) < U_i < u_B(t_i)$ : in this case, we have  $H_{B \cup \{v_j\}}(t_i) - H_B(t_i) = 0$ .

Meanwhile, we can derive that

$$H_{A \cup \{v_j\}}(t_i) - H_A(t_i)$$

$$= \min\{u_{A \cup \{v_j\}}(t_i), U_i\} - \min\{u_A(t_i), U_i\}$$

$$= \min\{u_{A \cup \{v_j\}}(t_i), U_i\} - u_A(t_i)$$

$$= \min\{u(t_i, v_i), U_i - u_A(t_i)\} \ge 0.$$

Thus we can obtain Equation (3).

(Case 3) If  $u_B(t_i) \leq U_i$ : in this case, we have  $H_{A \cup \{v_j\}}(t_i) - H_A(t_i) \\ = \min\{u_{A \cup \{v_j\}}(t_i), U_i\} - \min\{u_A(t_i), U_i\} \\ = \min\{u(t_i, v_j), U_i - u_A(t_i)\}$  and  $H_{B \cup \{v_i\}}(t_i) - H_B(t_i)$ 

 $\begin{aligned} H_{B\cup\{v_j\}}(t_i) - H_B(t_i) \\ &= \min\{u_{B\cup\{v_j\}}(t_i), U_i\} - \min\{u_B(t_i), U_i\} \\ &= \min\{u(t_i, v_j), U_i - u_B(t_i)\}. \end{aligned}$  For i.  $u(t_i, v_j) \leq U_i - u_B(t_i)$ , we have

 $H_{A\cup\{v_i\}}(t_i) - H_A(t_i) = u(t_i, v_i) = H_{B\cup\{v_i\}}(t_i) - H_B(t_i).$ 

For ii.  $U_i - u_B(t_i) < u(t_i, v_i) < U_i - u_A(t_i)$ , we have

$$\begin{split} &H_{A \cup \{v_j\}}(t_i) - H_A(t_i) \\ &= u(t_i, v_j) > U_i - u_B(t_i) = H_{B \cup \{v_i\}}(t_i) - H_B(t_i). \end{split}$$

For iii.  $U_i - u_A(t_i) < u(t_i, v_i)$ , we have

$$\begin{split} &H_{A \cup \{v_j\}}(t_i) - H_A(t_i) \\ &= U_i - u_A(t_i) \ge U_i - u_B(t_i) = H_{B \cup \{v_j\}}(t_i) - H_B(t_i). \end{split}$$

Therefore, we prove that H(X) is submodular.

Additionally, we need to point out that  $U(X, P^*)$  is not submodular, which can be proved using a counterexample.  $\blacksquare$  B. Surrogate Function Gap Analysis

Given the selected subset X, the optimal energy allocation  $P^*$  has the maximal task utility. In this subsection we would evaluate the task utility by applying our energy allocation strategy P' in the surrogate function H(X). Thus we begin to analyze the gap between U(X,P') and  $U(X,P^*)$ .

**Theorem 3:** For any sensor set X, the achieved overall task utility by using strategy P' in U(X,P') can reach at least 1/2 of the optimal task utility by using  $P^*$  in  $U(X,P^*)$ .

*Proof:* Assuming the selected subset X includes sensors  $\{v_{1'}, v_{2'}, ..., v_{|X|'}\}$ , where  $v_{j'}$  represents the j-th sensor in the fixed sequence of X. For our energy allocation strategy P', we denote the corresponding scheme by  $(X, P') = \{v_{1'}^{P'}, v_{2'}^{P'}, ..., v_{|X|'}^{P'}\}$ . Similarly, we denote the optimal scheme when applying the optimal energy allocation strategy  $P^*$  by  $(X, P^*) = \{v_{1'}^{P^*}, v_{2'}^{P^*}, ..., v_{|X|'}^{P^*}\}$ .

**Auxiliary scheme introduction:** To evaluate the utility gap between schemes (X, P') and  $(X, P^*)$ , we introduce two new schemes  $(Y, P' \& P^*)$  and  $(X_j, P' \& P^*)$ , respectively. Scheme  $(Y, P' \& P^*)$  includes a special sensor set Y with an associated energy allocation strategy  $(P' \& P^*)$ , which is denoted by

$$(Y,P'\ \&\ P^*)=\{v_{1'}^{P'},...,v_{|X|'}^{P'},v_{1'}^{P^*},...,v_{|X|'}^{P^*}\}.$$

We explain this special sensor set Y by assuming that we can select sensors in X twice. For the first |X| sensors, we utilize energy allocation strategy P' and for the second |X| sensors, we apply strategy  $P^*$  instead.

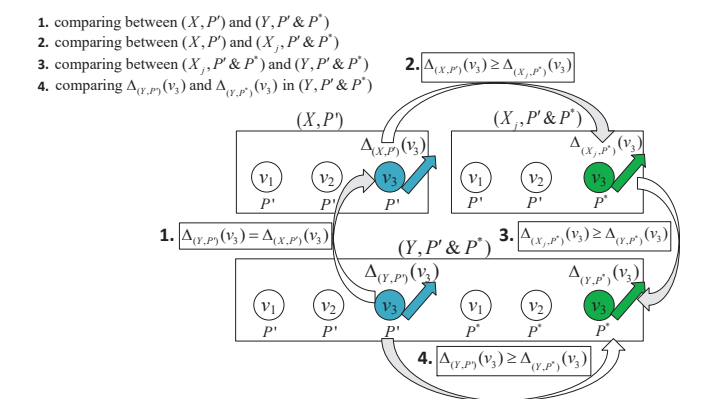


Fig. 4: A concrete example for marginal utility comparison

Scheme  $(X_j, P' \& P^*)$  includes the first j sensors of set X which is denoted by

$$(X_j, P' \& P^*) = \{v_{1'}^{P'}, v_{2'}^{P'}, ..., v_{(j-1)'}^{P'}, v_{j'}^{P^*}\}.$$

In this special scheme, the front j-1 sensors apply the aforementioned greedy strategy P' and the j-th sensor apply the optimal allocation strategy like scheme  $(X, P^*)$ .

**Marginal utility comparison:** Remember we allocate energy for various tasks by turns in the fixed sequence, we then define the marginal utility  $\Delta_{(X,P)}(v_{j'})$  for the energy allocation scheme (X,P) when a new sensor  $v_{j'}$  is added and placed at the end of the sequence. By this way, we have the marginal utility  $\Delta_{(X,P')}(v_{j'})$  and  $\Delta_{(X,P^*)}(v_{j'})$  for (X,P') and  $(X,P^*)$  respectively. Based on a series of definitions, we can achieve some equations.

1. Comparison between (X,P') and  $(Y,P' \& P^*)$ : Since scheme  $(Y,P'\&P^*)$  has different energy allocation strategies for the first and second |X| sensors, then we use  $\Delta_{(Y,P')}(v_{j'})$  and  $\Delta_{(Y,P^*)}(v_{j'})$  to denote their marginal utility independently. Apparently, we have

$$\Delta_{(X,P')}(v_{j'}) = \Delta_{(Y,P')}(v_{j'}). \tag{4}$$

**2.** Comparison between (X, P') and  $(X_j, P' \& P^*)$ : For the same reason, we use  $\Delta_{(X_j, P^*)}(v_{j'})$  to denote the marginal utility for scheme  $(X_j, P' \& P^*)$  when adding a new sensor  $v_{j'}$  where the optimal energy allocation strategy  $P^*$  is used. As we achieve the maximal utility for each single sensor using the greedy allocate energy strategy, we have

$$\Delta_{(X_i,P^*)}(v_{i'}) \le \Delta_{(X,P')}(v_{i'}).$$
 (5)

3. Comparison between  $(X_j,P'\&P^*)$  and  $(Y,P'\&P^*)$ : When considering the marginal utility  $\Delta_{(Y,P^*)}(v_{j'})$ , we can observe the current situation of energy allocation in  $(Y,P'\&P^*)$  as  $\{v_{1'}^{P'},...,v_{|X|'}^{P'},v_{1'}^{P^*},...,v_{j'}^{P^*}\}$ . Then current sensor set  $Y_j$  is  $\{v_{1'},v_{2'},...,v_{|X|'},...,v_{1'},...,v_{j'}\}$ . Meanwhile, we observe the situation of energy allocation in  $(X_j,P'\&P^*)$  as  $\{v_{1'}^{P'},...,v_{(j-1)'}^{P'},v_{j'}^{P^*}\}$ . Then current sensor set  $X_j$  is  $\{v_{1'},v_{2'},...,v_{j'}\}$ .

Obviously, we have  $X_j \setminus \{v_{j'}\} \subseteq Y_j \setminus \{v_{j'}\}$ . Similar to the proof of submodularity for surrogate function H(X), we can achieve that

$$\Delta_{(Y,P^*)}(v_{j'}) \le \Delta_{(X_i,P^*)}(v_{j'}).$$
 (6)

**4.** Comparison in  $(Y, P' \& P^*)$ : Combine Equation (4), (5) and (6), we have

$$\Delta_{(Y,P^*)}(v_{j'}) \le \Delta_{(Y,P')}(v_{j'}).$$
 (7)

A concrete example: We give a toy example to illustrate the definitions and above consequence as shown in Fig. 4. We consider the marginal utility when adding a new sensor  $v_3$  where  $\Delta_{(X,P')}(v_3)$  corresponds to scheme (X,P'),  $\Delta_{(X_j,P^*)}(v_3)$  corresponds to scheme  $(X_j,P' \& P^*)$ ,  $\Delta_{(Y,P')}(v_3)$  and  $\Delta_{(Y,P^*)}(v_3)$  corresponds to scheme  $(Y,P' \& P^*)$ . Finally we have the following equation as

$$\Delta_{(Y,P')}(v_3) = \Delta_{(X,P')}(v_3) \ge \Delta_{(X_i,P^*)}(v_3) \ge \Delta_{(Y,P^*)}(v_3).$$

Therefore, we can sum all the marginal utility in set Y and derive the result as follows:

$$OPT = \sum_{v_{j'} \in Y} \Delta_{(Y,P'\&P^*)}(v_{j'})$$

$$= \sum_{v_{j'} \in X} \Delta_{(Y,P')}(v_{j'}) + \sum_{v_{j'} \in X} \Delta_{(Y,P^*)}(v_{j'})$$

$$\leq 2 \sum_{v_{j'} \in X} \Delta_{(Y,P')}(v_{j'}) = 2 \sum_{v_{j'} \in X} \Delta_{(X,P')}(v_{j'})$$

$$= 2U(X,P') = 2H(X).$$

As a consequence, we prove that the constructed surrogate function H(X) can obtain at least 1/2 of the optimal solution.

# C. Approximation Ratio Analysis

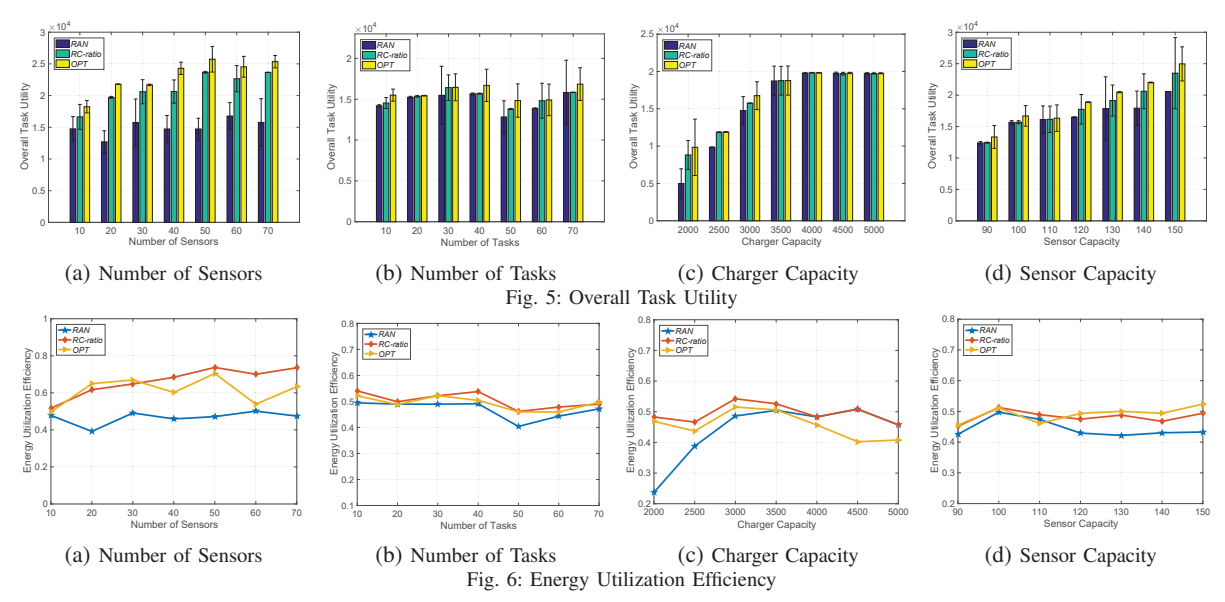
**Theorem 4:** The proposed RC-ratio algorithm has (1 - 1/e)/4 bi-criterion approximation guarantee with computational complexity bounded by  $O(m^2)$ .

*Proof:* From subsection V-A we have sufficient and specific theoretic analysis that the surrogate function is nonnegative, monotone and submodular. Meanwhile, the mobile charger energy budget is just a general routing constraint. Therefore our formulated problem can be regarded as one case of submodular optimization with routing constraints referring to [32]. By executing algorithm RC-ratio which adds sensors in the order of the marginal benefit per unit marginal energy cost, then we can achieve (1-1/e)/2 bi-criterion approximation ratio, comparing to the solution of the surrogate submodular function optimization with a slight relaxed budget constraint. The approximated cost function  $\hat{\mathcal{C}}(X)$  would directly influence the relaxed decree of budget constraint.

Furthermore, from subsection V-B we have proved the 1/2 gap between the optimal energy allocation and ours in H(X) when fixing the charging route. Therefore we can combine the two kinds of bounds above and obtain the final (1-1/e)/4 bi-criterion approximation guarantee. We know RC-ratio has at most m iterations. In each iteration, using the nearest neighbour rule to select the next sensor also cost at most m time, Thus the overall time complexity is bounded by  $O(m^2)$ .

# VI. NUMERICAL EVALUATIONS

In this section, we conduct extensive simulations under different network settings to evaluate the performance of our proposed algorithm and reveal insights about it.



#### A. Evaluation Setup

We assume these stationary rechargeable sensors with corresponding tasks to be executed are randomly distributed in a 100m\*100m 2D plane. The default number of sensors and tasks are 10 and 50 respectively. The task utility weights are uniformly distributed within the range [5,20]. By default, the task utility threshold is 2000, the energy capacity of the mobile charger and sensors are 3000 and 100 separately. The residual energy of sensors is uniformly distributed within the range [0,20]. We set  $\alpha=5$  and  $\beta=2$ .

# B. Baseline Setup

For effective and fair comparison, we introduce the random algorithm (RAN) and optimal algorithm (OPT) for comparison. We devise RAN using the random sensor selection with the greedy energy allocation strategy. Without exceeding the energy budget of the mobile charger, we randomly select partial sensors to charge and allocate energy greedily to the task which has the best weight. For OPT, we simply use a powerful optimization software called LINGO to help solve nonlinear integer programming. Although the CTMC problem has high computing complexity, we can still obtain the optimal solution for small instances of this problem. Based on the series of settings above, we run 10 times of different algorithms to average the results.

# C. Evaluation Results and Analysis

In general, the proposed RC-ratio outperforms RAN substantially and can achieve a near-optimal solution covering 84.9% of OPT at least, which validates the theoretical results. Moreover, RC-ratio can prompt the mobile charger to spend more energy charging for task execution to increase the overall network utility, rather than wasting energy on traveling.

1) Impact of the number of sensors: Our simulation results show that RC-ratio outperforms RAN on average by 40.6% and obtains at least 84.9% of the OPT as the number of sensors increases from 10 to 70. As shown in Fig. 5a, the achieved overall task utility of both RC-ratio and OPT increase monotonically with the sensor number while RAN algorithm

just fluctuates to keep stable. This is because the proposed RC-ratio always selects the most beneficial sensor. Then more sensors provide more chances for the mobile charger to select better closed tour and energy allocation strategy. However, more sensors would also introduce some 'good' or 'bad' sensors for RAN and cause fluctuations in overall task utility. Meanwhile, we can observe from Fig. 6a that RC-ratio and OPT spend 66.26% and 61.35% energy of the whole charger capacity, respectively, better than 44.6% in RAN, thus reflect better energy efficiency.

- 2) Impact of the number of tasks: Our simulation results show that RC-ratio outperforms RAN on average by 10.7% and obtains at least 88.8% of OPT as the number of tasks increases from 10 to 70. As shown in Fig. 5b, the achieved overall task utility of these algorithms do not increase with the task number. And Fig. 6b shows RC-ratio still has 50.1% energy utilization efficiency similar to OPT which has 50.6%, but better than RAN that has 44.1%. The reason accounts for these results is that when utility weight and charger capacity are fixed, RAN selects sensors randomly but allocates energy using the same strategy in RC-ratio, thus can exhibit good performance. Therefore, the number of tasks has little impact on the charging utility.
- 3) Impact of the charger capacity: Our simulation results show that RC-ratio outperforms RAN on average by 14.8% and obtains at least 89.6% of OPT as the charger capacity increases from 2000 to 5000. Fig. 5c shows that the achieved overall task utility of these three algorithms increases with the charger capacity from 2000 to 4000 but keeps stable from 4000 to 5000. We can explain that more energy provides more energy replenishment and improves the overall task utility. Each task has the utility threshold and thus the overall task utility would invariably increase until up to the threshold value. From Fig. 6c we observe RAN has the lowest energy utilization efficiency when the charger capacity is less than 3500, but OPT would be the lowest one instead when the charger capacity is more than 3500. RAN performs worse

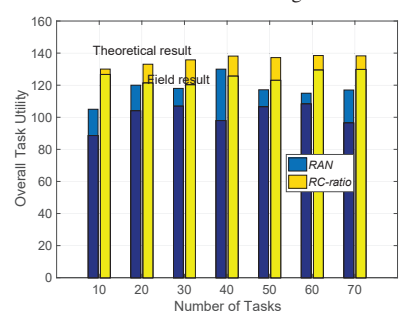


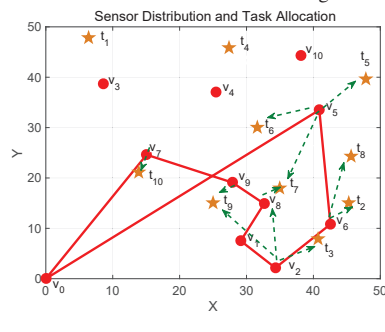
Sensor Mobile Charge

Fig. 7: Indoor office room

Sensor

Fig. 8: Outdoor soccer field





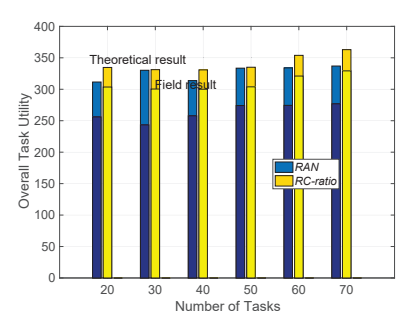


Fig. 9: Overall task utility for indoor scenario

Fig. 10: The traveling path

Fig. 11: Overall task utility for outdoor scenario

due to the random selection and neglect of the traveling cost. However, when increasing the charger capacity, OPT would try best to achieve the optimal task utility but not consider the energy efficiency. Finally, RC-ratio performs the best among all candidate algorithms.

4) Impact of the sensor capacity: Our simulation results show that RC-ratio outperforms RAN on average by 6.4% and obtains at least 93.2% of OPT as the amount of sensor capacity increases from 90 to 150. Fig. 5d shows the achieved overall task utility of these three algorithms increases almost linearly with the sensor capacity. Indeed, as the amount of sensor capacity increases, the mobile charger would replenish more power to these sensors for task execution. Without exceeding the task utility threshold, the achieved overall task utility would increase apparently. As shown in Fig. 6d, RC-ratio and OPT can keep better energy utilization efficiency at 48.3% and 49.1% respectively. However, RAN has 44.5% efficiency and strong fluctuation which decreases to 42%.

## VII. FIELD EXPERIMENT

To further evaluate our proposed algorithm, we conduct field experiments in both small (indoor) and larger (outdoor) scale environment as shown in Fig. 7 and Fig. 8.

## A. Experimental Setup

Fig. 7 shows our testbed consists of a TX91501 power transmitter produced by Powercast [33], rechargeable sensors and an AP connecting to a laptop to report the collected data from sensor nodes. Note that we install the transmitter on a robot car driven by Raspberry Pi for mobility. In the small scale environment, we place 10 rechargeable sensor nodes in the office room of a 5m \* 5m square area. In the large scale environment, we select the half soccer field region to place 20 sensors. The transmit power of TX91501 is set to

3W and added into the energy consumption model of the robot car. The received power is 40mW and the consuming power of the robot car is 4W running at a speed of 0.3m/s. The charging request of each sensor node is 1J. We define a utility computing model for tasks where the task utility weights are randomly distributed in the range [5, 20] and each task utility threshold is 20. Finally, we set the energy budget of the mobile charger 800J and 4000J for the indoor and outdoor environment, respectively.

# B. Experimental Results and Analysis

For indoor scenario, we can observe from Fig. 9 that the overall task utility of RC-ratio outperforms that of RAN by 23.6% at average and 42.9% at most when we increase the amount of tasks from 10 to 70. We can also see that the field results are much lower than the theoretical results. The reason is that when we conduct the field experiment, the receiving power of wireless energy transfer is lower than 40mW due to the impact of distances and angles. Meanwhile, we have to spend extra time adjusting the charging distance, angles and turning for the robot car, left less time/energy for wireless charging. For example, when a typical case where 10 sensors with associated 10 tasks is considered, we exhibit the actual traveling path for this field experiment, as shown in Fig. 10. We find that due to the energy budget of the mobile charger, sensors  $v_3, v_4$  and  $v_{10}$  would not be selected for energy transfer and tasks  $t_1, t_4$  and  $t_5$  would not be executed. However, we can still achieve fine task utility in the network.

The obtained result from the outdoor soccer field experiment is similar to that from the indoor field experiment (in Fig. 8). Our proposed RC-ratio outperforms RAN better but worse than the theoretical result for the above same reason. We can observe that the increase of charger capacity leads to the improvement of the overall task utility when comparing Fig. 9 with Fig. 11. Meanwhile, there are more energy costs on traveling when running in a large scale region.

# VIII. CONCLUSION

The key novelty of this paper is that we make the first effort towards the collaborated tasks-driven mobile charging which jointly considers sensors selection with energy allocation and charging tour scheduling. The key contribution of this paper is proposing a surrogate function with the greedy energy allocation strategy. Based on this scheme, we present the specific theoretical analysis and proof that the constructed function is submodular and can achieve at least 1/2 the value of optimal solution. We prove the formulated problem can be transformed into the problem of maximizing a monotone submodular function subject to a general routing constraint and utilizing our proposed algorithm can achieve (1-1/e)/4 approximation ratio. Our simulation and field experimental results show that the proposed algorithm achieves excellent performance which exhibits the near-optimality.

#### ACKNOWLEDGMENTS

Panlong Yang is the corresponding author. This research is partially supported by National key research and development plan 2017YFB0801702, NSFC with No. 61772546, 61625205, 61632010, 61751211, 61772488, 61520106007, Key Research Program of Frontier Sciences, CAS, No. QYZDY-SSW-JSC002, NSFC with No. NSF ECCS-1247944, and NSF CNS 1526638. NSF of Jiangsu For Distinguished Young Scientist: BK20150030, in part by the National Key R&D Program of China under Grant No. 2018YFB1004704, in part by the National Natural Science Foundation of China under Grant No. 61502229, 61872178, 61832005, 61672276, 61872173, and 61321491, in part by the Natural Science Foundation of Jiangsu Province under Grant No. BK20181251, in part by the Fundamental Research Funds for the Central Universities under Grant 021014380079.

#### REFERENCES

- L. Xie et al., "Wireless power transfer and applications to sensor networks," *IEEE Wireless Communications*, vol. 20, no. 4, pp. 140–145, 2013.
- [2] Y. Yang et al., Wireless rechargeable sensor networks. Springer, 2015.
- [3] H. Dai et al., "Wireless charger placement for directional charging," IEEE/ACM Transactions on Networking (TON), vol. 26, no. 4, pp. 1865– 1878, 2018.
- [4] S. Zhang et al., "P 3: Joint optimization of charger placement and power allocation for wireless power transfer," in 2015 IEEE Conference on Computer Communications (INFOCOM). IEEE, 2015, pp. 2344–2352.
- [5] L. Li et al., "Radiation constrained fair wireless charging," in Sensing, Communication, and Networking (SECON), 2017 14th Annual IEEE International Conference on. IEEE, 2017, pp. 1–9.
- [6] H. Dai et al., "Omnidirectional chargability with directional antennas," in Network Protocols (ICNP), 2016 IEEE 24th International Conference on. IEEE, 2016, pp. 1–10.
- [7] R. Dai et al., "Robustly safe charging for wireless power transfer," in IEEE INFOCOM 2018-IEEE Conference on Computer Communications. IEEE, 2018, pp. 378–386
- IEEE, 2018, pp. 378–386.
  [8] H. Dai et al., "Radiation constrained scheduling of wireless charging tasks," *IEEE/ACM Transactions on Networking*, vol. 26, no. 1, pp. 314–327, 2018.
- [9] N. Yu et al., "Placement of connected wireless chargers," in IEEE IN-FOCOM 2018-IEEE Conference on Computer Communications. IEEE, 2018, pp. 387–395.

- [10] Y. Peng et al., "Prolonging sensor network lifetime through wireless charging," in Real-time systems symposium (RTSS), 2010 IEEE 31st. IEEE, 2010, pp. 129–139.
- [11] C. Wang et al., "A mobile data gathering framework for wireless rechargeable sensor networks with vehicle movement costs and capacity constraints," *IEEE Transactions on Computers*, vol. 65, no. 8, pp. 2411– 2427, 2016.
- [12] Y. Shi et al., "On renewable sensor networks with wireless energy transfer," in *INFOCOM*, 2011 Proceedings IEEE. IEEE, 2011, pp. 1350–1358.
- [13] X. Liguang et al., "On traveling path and related problems for a mobile station in a rechargeable sensor network," in Fourteenth ACM International Symposium on Mobile Ad Hoc NETWORKING and Computing, 2013, pp. 109–118.
- [14] L. He et al., "Evaluating the on-demand mobile charging in wireless sensor networks," *IEEE Transactions on Mobile Computing*, vol. 14, no. 9, pp. 1861–1875, 2015.
- [15] Y. Pang et al., "Charging coverage for energy replenishment in wireless sensor networks," in Networking, Sensing and Control (ICNSC), 2014 IEEE 11th International Conference on. IEEE, 2014, pp. 251–254.
- [16] C. Lin et al., "mts: Temporal- and spatial-collaborative charging for wireless rechargeable sensor networks with multiple vehicles," in IN-FOCOM, 2018 Proceedings IEEE. IEEE, 2018, pp. 1350–1358.
- [17] L. Fu et al., "Minimizing charging delay in wireless rechargeable sensor networks," in *INFOCOM*, 2013 Proceedings IEEE, 2013, pp. 2922– 2930
- [18] W. Liang et al., "Approximation algorithms for charging reward maximization in rechargeable sensor networks via a mobile charger," IEEE/ACM Transactions on Networking, vol. 25, no. 5, pp. 3161–3174, 2017
- [19] R. N. Murty et al., CitySense: An Urban-Scale Wireless Sensor Network and Testbed, 2008.
- [20] M. Gruber et al., "Co 2 sensors for occupancy estimations: Potential in building automation applications," *Energy & Buildings*, vol. 84, no. 3, pp. 548–556, 2014.
- [21] S. Bhattacharya et al., "Multi-application deployment in shared sensor networks based on quality of monitoring," in *IEEE Real-Time and Embedded Technology and Applications Symposium*, 2010, pp. 259–268.
- [22] D. Zeng et al., "Energy minimization in multi-task software-defined sensor networks," *IEEE Transactions on Computers*, vol. 64, no. 11, pp. 3128–3139, 2015.
- [23] G. A. Shah et al., "Exploiting energy-aware spatial correlation in wireless sensor networks," in *International Conference on Communication Systems Software and Middleware*, 2007. Comsware, 2007, pp. 1–6.
- [24] F. Bouabdallah et al., "Reliable and energy efficient cooperative detection in wireless sensor networks," Computer Communications, vol. 36, no. 5, pp. 520–532, 2013.
- [25] Y. Wang et al., "Achieving full-view coverage in camera sensor networks," Acm Transactions on Sensor Networks, vol. 10, no. 1, pp. 1–31, 2013.
- [26] M. Zhao et al., "Joint mobile energy replenishment and data gathering in wireless rechargeable sensor networks," in Proceedings of the 23rd International Teletraffic Congress. International Teletraffic Congress, 2011, pp. 238–245.
- [27] P. Zhou et al., "Leveraging target k-coverage in wireless rechargeable sensor networks," in *Distributed Computing Systems (ICDCS)*, 2017 IEEE 37th International Conference on. IEEE, 2017, pp. 1291–1300.
- [28] Z. Dong et al., "Energy synchronized task assignment in rechargeable sensor networks," in Sensing, Communication, and Networking (SEC-ON), 2016 13th Annual IEEE International Conference on. IEEE, 2016, pp. 1–9.
- [29] S. Khuller et al., "The budgeted maximum coverage problem," Information Processing Letters, vol. 70, no. 1, pp. 39–45, 1999.
- [30] D. Feillet et al., Traveling Salesman Problems with Profits. INFORMS, 2005.
- [31] D. J. Rosenkrantz et al., "An analysis of several heuristics for the traveling salesman problem," in Fundamental Problems in Computing. Springer, 2009, pp. 45–69.
- [32] H. Zhang *et al.*, "Submodular optimization with routing constraints." in *AAAI*, vol. 16, 2016, pp. 819–826.
- [33] Powercast, "Online," http://www.powercastco.com/products/.